Traditional timber carpentry joints: monotonic tests and modeling

Artur O. Feio[1], José S. Machado[2]

Summary

The structural safety and behaviour of traditional timber structures depends significantly on the performance of their connections. The behaviour of a traditional mortise and tenon timber joint is addressed using physical testing of full-scale specimens. New chestnut wood and old chestnut wood obtained from structural elements belonging to ancient buildings is used. In addition, nonlinear finite element analysis is used to better understand the behaviour observed in the full-scale experiments, in terms of failure mode and ultimate load.

The results show that the failure mechanism and load-displacement diagrams observed in the experiments are well captured by the proposed non-linear finite element analysis, and the parameters that affect mostly the ultimate load of the timber joint are the compressive strength of wood perpendicular to the grain and the normal stiffness of the interface elements representing the contact between rafter and brace.

1. Introduction

In the past, timber structural design was dominated by carpenter know-how, resulting from tradition and empirical knowledge. With respect to traditional wood-wood joints, rules-of-thumb dominated the technology and the present knowledge is still rather limited. In the present work, a mortise and tenon joint, see Fig. 1, was selected because it is one of the most commonly used in ancient timber structures and a typical example of an interlocking joint, forming usually an "L" or "T" type configuration. The key problem found in these joints is the possible premature failure induced in the structure caused by large displacements in the joint.

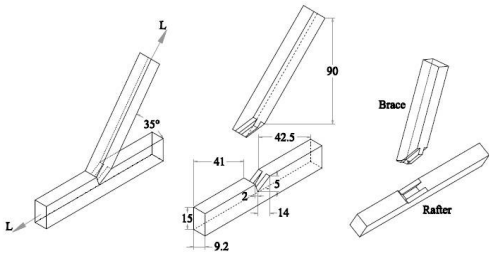

Fig. 1 Details of a typical tenon and mortise joint, with the geometry adopted in the testing program (dimensions in mm)

The bearing capacity of mortise and tenon joints is a function of the angle of the connection, and length of the toe and mortise depth. The lack of knowledge about this particular joint is determinant in the assessment of the load carrying capacity of existing wooden structures. Here, the objectives are to quantify the strength capacity of the joint by physical testing of full-scale specimens and to validate the adequacy of an anisotropic failure criterion to represent the behaviour of the joint by the comparison between experimental and numerical results.

The finite element method is adopted to simulate the structural behaviour and obtain a better understanding of the failure process observed in experimental tests. Calculations are performed using a plane stress continuum model and the failure criterion is based on multi-surface plasticity. Using the finite element model, the influence of compression perpendicular to the grain and elastic stiffness on the response is addressed in detail.

[1] Auxiliar Professor, Faculty of Architecture, University Lusíada, Portugal
[2] Research Officer, National Laboratory for Civil Engineering, Timber Structures Division, Portugal

2. Experimental Program

2.1 Description of test specimens

Chestnut wood (*Castanea sativa* Mill.) is usually present in historical Portuguese buildings and all the wood used in the test specimens came from the North of Portugal. In order to assess the influence of service time in the response, two groups were considered: New Chestnut Wood (NCW), obtained from recently sawn timber, and Old Chestnut Wood (OCW), obtained from structural elements belonging to ancient buildings (date and precise origin unknown) with unknown load history. The old logs were obtained from rehabilitation works and were provided by a specialist contractor claiming that the wood has been in service for over 100 years.

2.2 Ultimate force and failure patterns

Table 1 shows the results of the tests in terms of ultimate force (ranging between 121.6 kN up and 161.5 kN). Even if the number of specimens is rather low, the average force in terms of groups NCW and OCW exhibits only a marginal difference.

The compressive damage in the brace occurred either localized at the toe or distributed along the full contact length. Often, out-of-plane bulging of the rafter under the contact length was observed. In some cases, compressive damage was accompanied with shear failure in the rafter in front of the toe. Fig. 2 illustrates the typical damages observed at ultimate load. The specimens were produced avoiding the presence of large defects although accepting small defects.

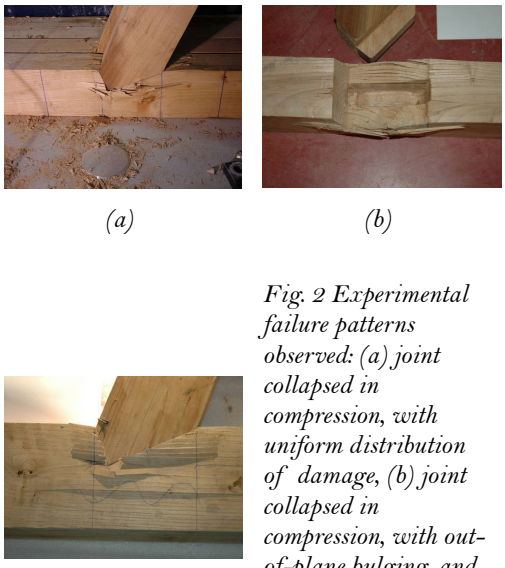

(a) *(b)* *(c)*

Fig. 2 Experimental failure patterns observed: (a) joint collapsed in compression, with uniform distribution of damage, (b) joint collapsed in compression, with out-of-plane bulging, and (c) combined failure in compression and shear parallel to the grain at the toe

2.3 Load-displacement diagrams

The envelope of all tests in terms of load-displacement diagrams is given in Fig. 3. In a first phase, the diagrams exhibit a nonlinear response, which is due to the adjustment of the tenon and the mortise.

It is noted that unloading-reloading cycles within working stress levels provide a constant stiffness, which is higher than the loading stiffness. The justification of this behavior is attributed to the nonlinear behavior of the interface between rafter and brace, which exhibits a closure phenomenon. Finally, after the ultimate force the displacement increases rapidly with a much lower stiffness, due essentially to the compressive failure of the wood in the rafter around the joint.

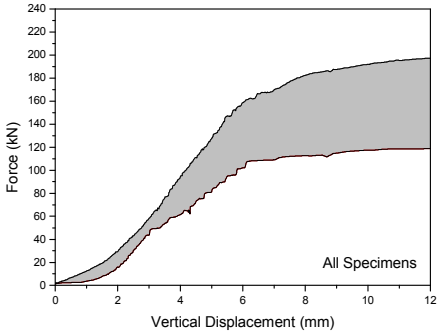

Fig. 3 Envelope of load- absolute displacement of the brace diagrams

3. Numerical Simulation

In order to further discuss the experimental results, a finite element simulation of the tests has been carried out and continuum quadratic elements (8-noded) were used to represent the wood and to represent the line interface between rafter and brace quadratic elements (6-noded) were used.

The integration schemes used are 2x2 Gauss integration points for the continuum elements and 3 Lobatto integration points for the interface elements. The simulations have been carried out using a globally convergent solution process, combining a Newton-Raphson method with arc-length and line search. The adopted failure criterion for wood consists of an extension of conventional formulations for isotropic quasi-brittle materials to describe orthotropic behaviour. It is based on multi-surface plasticity, including a Hill yield criterion for compression and a Rankine yield criterion for tension, and having different strengths in the directions parallel and perpendicular to the grain, see Lourenço *et al.* (1997) for details.

In the present case, the tensile part of the yield criterion was ignored due to the irrelevant contribution of the tensile strength in the global behaviour of the joint. This means that the yield surface reduces to the standard Hill criterion in compression. The adopted elastic and inelastic materials properties are detailed in Table 2 and have been obtained from a testing program aiming at characterizing chestnut, see Lourenço *et al.* (2007) and Feio (2006).

Table 1: Test results: ultimate force

	Ultimate Force (kN)	Average	Std. Dev.	Group
J_1	121.6	145.4	18.9	NCW
J_2	161.5			
J_3	159.7			
J_4	138.9			
J_5	126.4	145.5	16.7	OCW
J_6	157.1			
J_8	153.0			

Table 2: Adopted elastic and inelastic material properties

E_x	E_y	G_{xy}
$800\ N/mm^2$	$8500\ N/mm^2$	$1500\ N/mm^2$
$f_{c,x}$	$f_{c,y}$	β
$7\ N/mm^2$	$45\ N/mm^2$	-1.0

3.1 Numerical vs. experimental results

A structured mesh is used for the rafter and the brace, whereas an irregular transition mesh is used in the vicinity of the connection between rafter and brace. Interface elements are also used between the rafter and the brace. The thickness ranges from 62 mm to 93 mm, as shown in Fig.4. This aims at representing the thickness of the mortise.

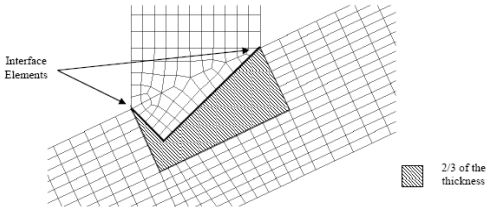

Fig. 4 Localization of the interface elements

The comparison between numerical and experimental load-displacement diagrams is given in Fig. 5. A first conclusion is that the stiffness of the interface elements has considerable influence on the yield strength of timber joints. In Fig. 5, three distinct situations are presented:

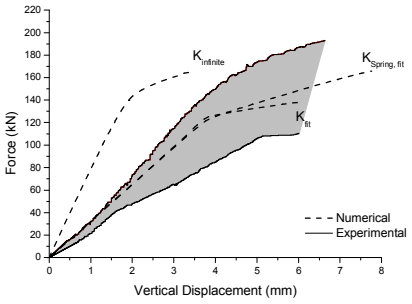

Fig. 5 Comparison between numerical and experimental load-displacement diagrams

- a numerical simulation with infinite stiffness of the interface elements in the normal direction, *kn*, and shear direction, *ks* ($k_{\text{infinite}} = k_n = k_s = 10^9$ N/mm^3);
- a numerical simulation with an adjusted stiffness of the interface elements obtained by inverse fitting of the experimental results (*kfit*), assuming that the shear and normal stiffness are related via the

Poisson's coefficient ν by $k_s = k_n / 2/(1+\nu)$; $k_n = 6000\ \mathrm{N/mm^3}$ and $k_s = 2308\ \mathrm{N/mm^3}$;

- a numerical simulation with a spring ($k_{spring} = 10^6$ N/m) located in the brace to simulate the reaction cell used in the experimental sets. The stiffness of the spring was again obtained by inverse fitting of the experimental results, keeping the adjusted stiffness of the interface elements.

The numerical results, in terms of force-displacement diagrams, with the adjusted stiffness for the interface elements, provide very good agreement with the experimental results both in the linear and nonlinear parts.

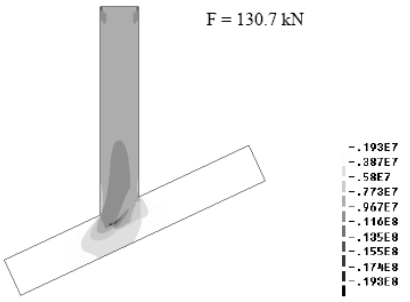

Fig. 6 Minimum principal stresses (values in N/m²) at ultimate load

A more relevant conclusion is that the usage of infinite stiffness for the interface (rigid joint) results in an increase of the slope of the first part of the response, from 30 kN/mm to 80 kN/mm (+ 266.7%). The ultimate force of the joint, given by an offset of the linear stretch by 2% in terms of strain values, also changes from 130 kN to 152 kN (+ 17%), once the joint becomes fully rigid.

Fig. 6 shows the contour of minimum principal stresses at ultimate load. It is possible to observe a concentration of stresses in a narrower band with peak stresses at the joint (zone where the interface elements were placed), upon increasing loading. As observed in the experiments, failure is governed by wood crushing, being the compressive strength of the wood, in the direction perpendicular to the joint, exhausted at failure.

4. Sensitivity study

A strong benefit of using numerical simulations is that parametric studies can be easily carried out and the sensitivity of the response to the material parameters can be easily evaluated. This allows a better understanding of the structural response.

The influence of the key parameters of the model in the response will be analyzed separately. The values k_n (normal stiffness of the interface), k_s (tangent stiffness of the interface), E_x and E_y (Young's moduli in the directions parallel and perpendicular to the grain, respectively) are assumed to be less well known and variations of 50% and 100% are made. f_x and f_y (compressive strengths in the directions parallel and perpendicular to the grain, respectively) are assumed to be well known and variations of +25% and -25% are made, corresponding to 0.75 and 1.25 times the initial value.

4.1 Normal and tangential stiffness of the interface

Fig. 7a shows a comparison between the results of the variation of the normal joint stiffness: with a reduction of 50% in k_n, the ultimate force of the joint, given by an offset of the linear stretch by 2%, decreases from 127.2 kN to 120 kN (-6%). Multiplying k_n by a factor of 2 the ultimate force of the joint, given by an offset of the linear stretch by 2%, increases from 127.2 kN to 135.0 kN (+7%).

The reduction/increase of the normal stiffness of the interface also affects the global stiffness of the joint; the global stiffness of the joint decreases as the normal stiffness of the interface decreases, being more sensitive to this variation when compared with the ultimate force. The reduction of 50% of the k_n parameter, results in a decrease of the slope of the first part of the response, from 32 kN/mm to 26 kN/mm (-23%). On the other hand, the multiplication by a

factor of 2 of this parameter results in an increase of the slope of the first part of the response, from 32 kN/mm to 41 kN/mm (+ 28%).

Fig. 7b shows a comparison between the results of the variation of the *ks* parameter. The ultimate force is insensitive to a *ks* variation, whereas the reduction/increase of the *ks* parameter affects the global stiffness of the joint: the global stiffness of the joint decreases as the *ks* parameter decreases. The reduction of 50% of the *ks* parameter, results in a decrease of the slope of the first part of the response, from 32 kN/mm to 28 kN/mm (-14%). On the other hand, the multiplication by a factor of 2 of this parameter results in an increase of the slope of the first part of the response, from 32 kN/mm to 37 kN/mm (+16%).

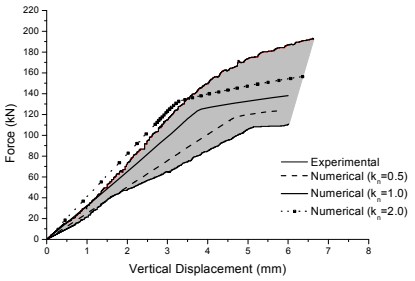

(a)

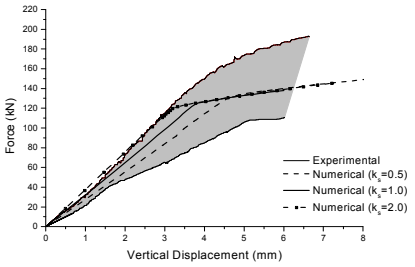

(b)

Fig. 7 – Effect of the variation of parameter: (a) k_n, and (b) k_s on the model response

4.2 Elastic modulus

The effect of the variation of the modulus of elasticity parallel and perpendicular to the grain was considered individually. The ultimate force is almost insensitive to the variation of the elastic modulus for wood (± 4%), in both considered directions. The inclusion of the effects of the elastic modulus does change significantly the elastic stiffness of the joint.

4.3 Compressive strength

The ultimate force and the global stiffness of the joint are insensitive to the variation of the compressive strength of wood in the direction parallel to the grain. Fig. 8 indicates the sensitivity of the ultimate force of the joint to the variation of the compressive strength of wood in direction perpendicular to the grain, as expected: with a reduction of 0,75, the ultimate force of the joint, given by an offset of the linear stretch by 2‰, decreases from 130 kN to 100 kN (-30%); multiplying by a factor of 1.25 the ultimate force of the joint, given by an offset of the linear stretch by 2‰, increases from 130 kN to 160 kN (+23%). However, the global stiffness of the joint is insensitive to the variation of the compressive strength perpendicular to the grain.

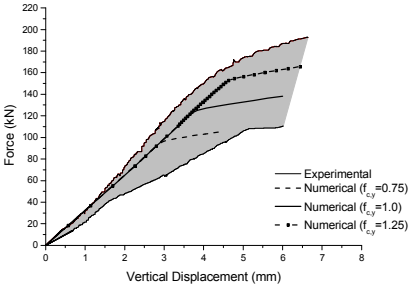

Fig. 8 – Effect of the variation of parameter k_s on the model response

5. Conclusions

Despite the wide use of mortise and tenon joints in existing timber structures scarce information is available for design and in situ assessment. The objective of the present study was to quantify the strength capacity of a wood-wood mortise and tenon joint by physical testing of full-scale specimens. In addition, the adequacy of an anisotropic failure criterion to represents the behaviour of a traditional mortise and tenon joint was assessed from the comparison between experimental and numerical results.

Two different wood groups have been used, one from new logs and another one from old logs

(date, precise origin and load history unknown). Reducing the defects to a minimum, no influence could be attributed to service time. Thus, safety assessment of new timber structures, made from old or new wood elements, can be made using similar mechanical data.

The failure mechanism and load-displacement diagrams observed in the experiments are well captured by the used non-linear finite element analysis. Nevertheless, the normal stiffness of the interface has considerable influence in the yield strength and deformation of timber joints. The parameters that affect mostly the ultimate load of the timber joint are the compressive strength of wood perpendicular to the grain and the normal stiffness of the interface elements representing the contact between rafter and brace. The tangential stiffness of the interface and the Young's moduli of wood have only very limited influence in the response. The compressive strength of wood parallel to the grain has no influence in the response.

References

[1] CEN, *EN 26891 – Timber structures. Joints made with mechanical fasteners general principles for the determination of strength and deformation characteristics.* European Committee for Standardization, Brussels, Belgium, 1991.

[2] CEN, *EN 408 – Timber structures. Structural timber and glued laminated timber. Determination of some physical and mechanical properties.* European Committee for Standardization, Brussels, Belgium, 2003.

[3] Eckelman, C., Haviarova, E., Rectangular mortise and tenon semirigid joint connection factors. *Forest Products Journal*, 58(12), pp. 49-55, 2008.

[4] Feio, A., Inspection and diagnosis of historical timber structures: NDT correlations and structural behaviour, *PhD Thesis, University of Minho, Portugal.* Available from www.civil.uminho.pt/masonry, 2006.

[5] Lourenço, P., De Borst, R., Rots, J., A plane stress softening plasticity model for orthotropic materials, *Int. J. Numerical Methods in Engineering*, 40, p. 4033-4057, 1997.

[6] Palma, P., Cruz, H. (2007), Mechanical behaviour of traditional timber carpentry joints in service conditions - results of monotonic tests. In From material to Structure – Mechanical behaviour and failures of the timber structures XVI International Symposium, Venice, Italy. ICOMOS IWC.